Available online at www.sciencedirect.com
ScienceDirect
Optics Communications 281 (2008) 141–145
OPTICS COMMUNICATIONS
www.elsevier.com/locate/optcom

Passive stabilization of a passively mode-locked Nd:$GdVO_4$ laser by inverse saturable absorption

Jiying Peng [a,b,*], Jieguang Miao [a,b], Yonggang Wang [c], Baoshan Wang [a,b], Huiming Tan [a], Longsheng Qian [a], Xiaoyu Ma [c]

[a] Changchun Institute of Optics, Fine Mechanics and Physics, Chinese Academy of Sciences, Changchun 130033, China
[b] Graduate School of Chinese Academy of Sciences, Beijing 100080, China
[c] Institute of Semiconductors, Chinese Academy of Sciences, Beijing 100083, China

Received 29 January 2007; received in revised form 23 August 2007; accepted 4 September 2007

Abstract

A diode-pumped Nd:$GdVO_4$ laser mode-locked by a semiconductor saturable absorber and output coupler (SESAOC) is passively stabilized to suppress Q-switched mode-locking. A phase mismatched BIBO second-harmonic generation (SHG) crystal is used for passive stabilization. The continuous wave mode-locking (CWML) threshold is reduced and the pulse width is compressed. The pulse width is 6.5 ps as measured at the repetition rate of 128 MHz.

Keywords: Passive stabilization; Mode locked laser; SESAOC; BIBO crystal

1. Introduction

Over the past decade, since the semiconductor saturable absorber mirrors (SESAMs) were successfully developed, there has been a great interest in the investigation of passively mode-locked solid-state lasers for the generation of ultra fast pulses [1,2], owing to their attractive applications in many fields and their advantages of compactness flexibility, and a wide spectrum ranging from the visible to the infrared. The semiconductor saturable absorber mirror (SESAM) has been well established as a useful device for passive mode-locking of many kinds of solid-state lasers [3–6]. The main reason for this device's utility is that both the linear and nonlinear optical properties can be engineered over a wide rang and the main absorber parameter can be custom designed for stable continuous wave (CW) mode-locking. In general, the SESAM is mostly used as an end mirror of a standing-wave cavity, which can lead to a higher complexity of the laser setup. Therefore, it is expected that a SESAM devices should simultaneously function as a saturable absorber and as an output coupler. Recently, the low temperature grown $In_{0.25}Ga_{0.75}As$ has been demonstrated to be an effective device for the dual functionality. Many lasers have been successfully mode-locked by this device [7–9]. In this paper a similar device was used as the mode-locking saturable absorber and output coupler.

The passive mode-locking stability in solid-state lasers is usually affected by passive Q-switching because of the higher upper state lifetime of the gain medium and consequently the laser starts to oscillate in Q-switched and mode-locked (QML) regime [10]. The QML regime is usually undesired because of the large amplitude and repetition rate fluctuations of the pulse train. In order to ensure suppression of Q-switched mode-locking instability, we should increase the pulse energy to exceed the critical threshold. In this case, the absorber may be damaged, especially for the laser crystal with small emission cross-section.

* Corresponding author. Address: Changchun Institute of Optics, Fine Mechanics and Physics, Chinese Academy of Sciences, Changchun 130033, China.
E-mail address: jiyingpeng111@163.com (J. Peng).

0030-4018/$ - see front matter © 2007 Elsevier B.V. All rights reserved.
doi:10.1016/j.optcom.2007.09.001

The semiconductor can to some extent be designed to match the laser material parameters and the operating conditions of a constructed laser. These methods however, can compromise the final performance of the device and have only a limited effect. Clearly, ways to expand the parameter range for CW mode-locking of existing and newly developed laser materials are necessary to extend further the parameters of the laser output.

It was recently shown that Q-switching instabilities in mode-locked lasers can be effectively suppressed by the introduction of an inverse saturable absorption. A diode-pumped Nd:$KGd(WO_4)_2$ laser mode-locked by a saturable Bragg mirror reflector (SBR) was successfully stabilized to suppress Q-switched mode-locking with an indium phosphide plate [11], and a second-harmonic generation (SHG) LBO crystal was used to stabilize an Nd:BaY_2F_8 laser mode-locked by a semiconductor absorber mirror (SAM) [12]. In this experiment, a diode-pumped Nd:$GdVO_4$ laser mode-locked by an SESAOC was demonstrated and the laser was successfully stabilized by a BIBO SHG crystal. The Q-switched mode-locking instability was suppressed and the CWML threshold was reduced. Especially, the pulse duration was shortened by use of a phase mismatched SHG crystal. To our knowledge, this is the first demonstration of a SESAOC mode-locked Nd:$GdVO_4$ laser stabilized by a BIBO SHG crystal.

2. Theoretical analysis

The condition for stable CW mode-locking is given [10]:

$$E_p^2 > E_{L,sat} E_{A,sat} \Delta R \tag{1}$$

Here, E_p is the intracavity pulse energy, $E_{L,sat} = h\upsilon A_L / N\sigma_L$ is the effective saturation energy of the laser medium, A_L is the mode area in the laser medium, N is the number of passes through the gain medium per cavity round trip, σ_L is the emission cross-section of the laser medium, $E_{A,sat} = F_{A,sat} A_A$ is the saturation energy of the saturable absorber, $F_{A,sat}$ is the saturation fluence of SESAOC, A_A is the mode area in the SESAOC, and ΔR is the saturable absorber modulation depth, which represents the total amount of saturable losses. In our case, the saturation energy of the laser medium is relatively high compared with those of other media employed for picosecond CW mode-locking because of the smaller emission cross-section of Nd:$GdVO_4$; moreover the saturable losses of the SESAOC is higher than the normal SESAM. Eq. (1) yields a high critical energy for the CW mode-locking.

To decrease the threshold for stable CW mode-locking operation we introduced close to the SESAOC a 1.5 mm long type-I BIBO crystal, cut for SHG at 1063 nm and antireflection coated on both sides. In fact, as shown in Ref. [13], the critical energy required for starting CW mode-locking can be reduced significantly in the presence of inverse saturable absorption such as two-photo absorption, free-carrier absorption, and SHG. In the nonsolitonic regime, this applied to the Nd:$GdVO_4$ laser, the critical energy becomes to be

$$E_p = \left(\frac{E_{A,sat} \Delta R}{2\tilde{\beta} + \frac{1}{E_{L,sat}}} \right)^{1/2} \tag{2}$$

Here, $\tilde{\beta} = \beta l / 3 A_{A,eff} \tau$ is the inverse saturable absorption coefficient related to SHG, l is the length of the SHG crystal, and $A_{A,eff}$ is the effective beam area in the SHG crystal, τ is the pulse duration. The parameter $\beta = 4\pi^2 Z_0 d_{eff}^2 l / n^3 \lambda_\omega^2$ includes the effective SHG coefficient d_{eff}, the fundamental wavelength λ_ω, and the refractive index n (Z_0 is the vacuum impedance).

Eq. (2) is valid for perfect phase matching. When the mismatched SHG crystal for the SPM is used, the Eq. (2) has to be modified. In our opinion, an SHG efficient coefficient $\eta = \sin c^2(\Delta k l / 2\pi)$ should be introduced to the Eq. (2). Therefore, for mismatching the Eq. (2) can be denoted to be

$$E_p = \left(\frac{E_{A,sat} \Delta R}{2\eta\tilde{\beta} + \frac{1}{E_{L,sat}}} \right)^{1/2} \tag{3}$$

For SESAOC with ΔR of 3%, $F_{A,sat}$ of 90 μJ/cm^2, the 50 μm mode radii in the absorber implies $E_{A,sat} = 7$ nJ. For Nd:$GdVO_4$ with an emission cross-section at 1063 nm of 7.6×10^{-19} cm^2, the 170 μm mode radii in the laser crystal implies $E_{L,sat} = 112$ μJ. Thus, Eq. (1) predicts a critical energy of $E_p = 0.153$ μJ. For BIBO SHG crystal, where the mode radii in the crystal $A_{A,eff} \approx 50$ μm, $l = 2$ mm, $d_{eff} = 2.96$ pm/V, $n = 1.6$, $\lambda_\omega = 1063$ nm, $Z_0 = 377\ \Omega$, and assuming a pulse duration of 10 ps, the Eq. (3) predicts

$$E_p = \left[\frac{2.12}{\sin c^2\left(\frac{\Delta k l}{2\pi}\right) \times 98 + 0.9} \right]^{\frac{1}{2}} \times 10^{-7}\ (\mathrm{J}) \tag{4}$$

According to Eq. (4), we can plot the critical pulse energy E_p dependence of the phase-mismatch $\Delta k l/2$. Fig. 1 shows the behavior of the critical pulse energy E_p as a function of the phase-mismatch $\Delta k l/2$.

To stabilize the mode-locking pulse and simultaneously decrease the pulse duration, a phase mismatched SHG crystal should be used in the Nd:$GdVO_4$ laser, because the phase mismatched SHG crystal can introduce the self-phase modulation (SPM) [14], which broadens the pulse spectrum. Generally, the SHG inverse saturable absorption is responsible for the pulse stabilization and the SPM is related to the pulse shortening. But strong SHG absorption can introduce more losses and reduce the modulation depth ΔR of the semiconductor absorber, it will broaden the mode-locking pulses or results in the generation of multiple pulses. Excessive SPM also is not needed because of the pulse breakup. So for perfect stable CW mode-locking with short pulses, the SHG and the SPM must be carefully balanced. Near perfect phase

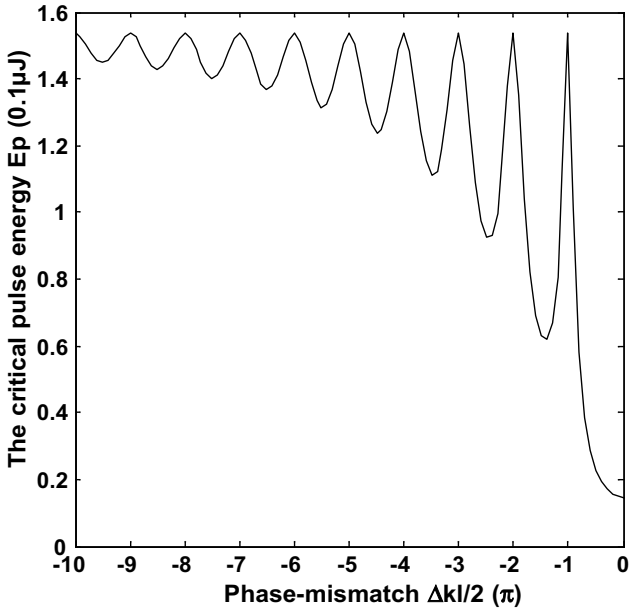

Fig. 1. The critical pulse energy as a function of phase mismatch.

matching ($\Delta k \approx 0$) the SHG effectively stabilizes the CW mode-locking but increases the pulse duration significantly, flattening the pulse shape [12]. Increasing phase mismatch Δk leads to stronger SPM, which eventually destabilizes the mode-locking because of pulse breakup. When Δk is increased further, both SPM and SHG inverse absorption decreases, permitting stable CW mode-locking with short pulses. However, the SHG inverse absorption cannot decrease to zero or very weak, otherwise the Q-switching instability cannot be suppressed significantly. When $\frac{1}{2}\Delta kl \approx m\pi$ $(m = -1, -2, -3, \ldots)$, the inverse saturable absorption is minimized so that only SPM contributes to the mode-locking process though phase-locking. In this case we can get the shortest pulse width, but the SHG inverse saturable absorption becomes too weak to influence the laser operation any more and the Q-switched mode-locking cannot be suppressed significantly. When $\frac{1}{2}\Delta kl \approx (m + \frac{1}{2}\pi)$ $(m = -1, -2, -3, \ldots)$ or near the special range, the SHG inverse saturable absorption and the SPM both have the moderate value. In this case, we can get shorter pulse and the Q-switched mode-locking can be suppressed effectively. To well balance the SHG inverse absorption and the SPM, we consider that the $\frac{1}{2}\Delta kl \approx (m + \frac{1}{2}\pi)$ condition is the better choice for the mode-locking lasers. In order to compensate for the spectral blue-shifting [15] and hence improve the mode-locking processes, a SHG crystal with a negative phase-mismatch will need to generate red spectral components mainly on the leading edge of the pulse [16]. In this experiment, to validate the theoretical analysis two mismatched SHG crystals with $\frac{1}{2}\Delta kl = -2.5\pi$ and -3π were used for the pulse stabilization and pulse shortening. From Eq. (2) and Eq. (3) we know that d_{eff} is a vital parameter for the passive stabilization. So we selected the BIBO crystal as the SHG device because of its high effective SHG coefficient ($d_{\text{eff}} = 2.96$ pm/V). Owing to the high effective SHG coefficient the short BIBO crystal can get the same nonlinearity to that of longer LBO ($d_{\text{eff}} = 0.83$ pm/V). Furthermore, the very short BIBO SHG crystal can effectively reduce the GVM (group velocity mismatch); it is important for the mode-locking laser because the GVM is an unwanted phenomenon due to the pulses broadening.

3. Experimental setup and results

The cavity configuration is shown in Fig. 2. The Nd^{3+} concentration of the laser crystal was 0.5 at.%, and its length was 5 mm. The laser crystal was wrapped with indium foil and mounted in a copper block cooled by a thermo-electric cooler. One side of the laser crystal was coated antireflection for 808 nm ($T > 98\%$) pump wavelength and high reflection ($R > 99.8\%$) for the 1063 nm lasing radiation, the other side was coated antireflection for 1063 nm. The pump source was 8 W fiber-coupled laser diode with a core diameter of 0.4 mm and a numerical aperture of 0.22. The fiber output was focused into the laser crystal and the pump spot radius was about 200 μm. The resonator consisted of two highly reflective (at 1063 nm and 532 nm) mirrors, M1 and M2; one partially reflective (PR) mirror, SESAOC; a laser crystal; and an SHG crystal. The radii of curvature for M1 and M2 are 600 and 200 mm, respectively. The transmission rate of the SESAOC (at 1063 nm) is about 6%. Considering the thermal lens effect of the laser crystal, the cavity was designed to easily allow mode matching with the pump beam and to provide the proper spot size in the SESAOC. The total cavity length was about 1170 mm. M1 and M2 were separated by about 680 mm, the crystal and M1 were separated by about 100 mm. The SHG crystal was placed close to the output coupler. The mode radii in the crystal was about 170 μm and the mode radii in the SESAOC was approximately 50 μm. The SESAOC was simply mounted on a copper heat sink, but no active cooling was applied.

In the first part of the experiment, the mode-locking performance was studied by using only the SESAOC, and the BIBO SHG crystal was not used. The oscillation threshold was about 1.55 W. Near oscillation threshold the output was effectively CW; slightly increasing the pump power initiated a Q-switched mode-locked (QML) state. The tempo-

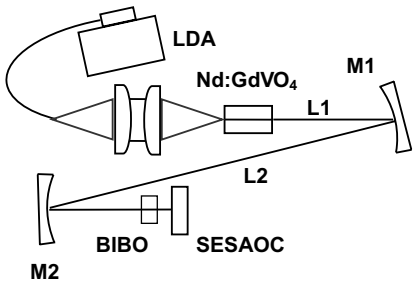

Fig. 2. Configuration of mode-locked Nd:$GdVO_4$ laser with the SESAOC and BIBO SHG crystal.

ral behavior of laser pulses was recorded by a fast response InGaAs photodiode with a time resolution of 0.5 ns and a LeCroy oscilloscope (9361C). The repetition rate of the Q-switched envelope increased from 200 to 460 kHz as the incident pump power increased from 2.5 to 6.8 W. The pulse width of the Q-switched envelope was about 0.5 μs. When the pump power increased to be about 7 W, the QML state is transformed into a CW mode-locked (CML) state. The repetition rate was about 128 MHz. At 7 W pump power, the average output power was about 1.38 W and the corresponding intracavity pulse energy was calculated to be about 0.174 μJ. At the maximum incident pump power of 8 W, 1.6 W average output power was obtained. The optical–optical conversion efficiency was about 20%. At 8 W pump power, the pulse width of the CW mode-locked laser output was measured by a home-made autocorrelator with a 3 mm long KTP crystal under type-II phase matched second-harmonic interaction in a collinear configuration. The pulse width was about 11 ps by assuming a Gaussian pulse shape. No damage to the SESAOC was observed over several hours of operation, which indicated a high damage threshold of the SESAOC.

In the second part of the experiment, a 1.5 mm long type I BIBO crystal, cut for SHG at 1063 nm and antireflection coated on both sides was inserted into the laser cavity, which introduced an inverse saturable absorption. The BIBO was placed closed to the SESAOC. Near oscillation threshold the output was also CW operation; slightly increasing the pump power initiated a Q-switched mode-locked (QML) state. When the pump power increased to be about 4.4 W, the QML state is transformed into a CW mode-locked (CML) state. At 4.4 W pump power, the average output power was about 0.52 W and the corresponding intracavity pulse energy was calculated to be about 0.066 μJ. Here, the pulse duration was measured to be about 100 ps. Thus, Eq. (1) predicts a critical energy of $E_p = 0.058$ μJ. The threshold for CW mode-locking is obviously lower than that without the SHG crystal. At 8 W pump power, the pulse width of the CW mode-locked laser output was measured by the same autocorrelator. The pulse width was about 23 ps by assuming a Gaussian pulse shape, which was much longer than that without SHG crystal.

In the third part of the experiment the phase matched ($\frac{1}{2}\Delta kl \approx 0$) SHG crystal was replaced to be the phase mismatched ($\frac{1}{2}\Delta kl = -2.5\pi, -3\pi$) crystals. The lengths of the two crystals both were 2 mm. The phase mismatched SHG crystal ($\frac{1}{2}\Delta kl = -2.5\pi$) introduced both the inverse saturable absorption and the SPM. At about 5.3 W incident pump power, the Q-switched pulse train was transformed into a CW mode-locked state. At 5.3 W pump power, the average output power was about 0.68 W and the corresponding intracavity pulse energy was calculated to be about 0.086 μJ. Here, the pulse duration was measured to be about 10 ps. Thus, Eq. (1) predicts a critical energy of $E_p = 0.092$ μJ. Fig. 3 shows the pulse train states without the SHG crystal and with it at 6 W pump power. The behavior of laser average output power as a function of the incident pump power was investigated as shown in Fig. 4. The maximum average output power was 1.26 W;

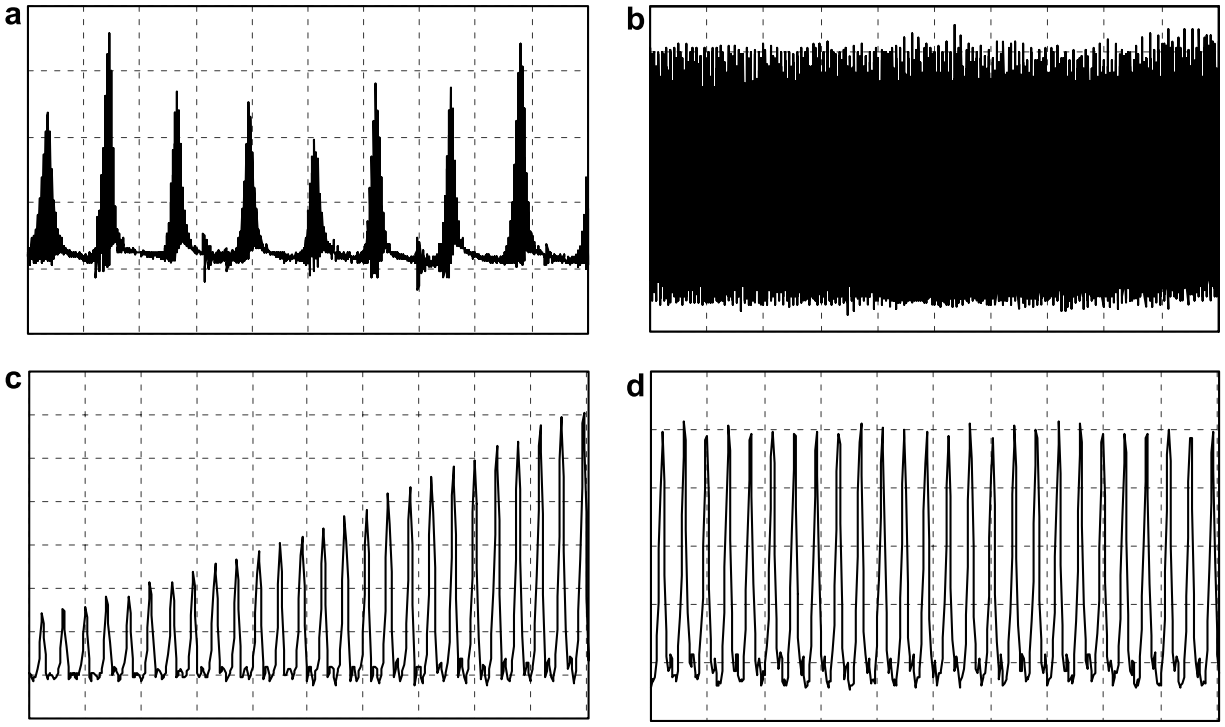

Fig. 3. The mode-locking pulse train with the passive stabilization and without it at 6 W pump power. (a) The pulse train only with the SESAOC (2 μs/div). (b) The pulse train with the SESAOC and BIBO crystal (2 μs/div). (c) The pulse train only with the SESAOC (20 ns/div). (d) The pulse train with the SESAOC and BIBO crystal (20 ns/div).

corresponded to an optical–optical conversion efficiency of about 16%. The pulse width was measured to be about 6.5 ps by assuming a Gaussian pulse shape, which is shorter than that without the phase mismatched SHG crystal. The autocorrelation trace is shown in Fig. 5. With the other mismatched SHG crystal ($\frac{1}{2}\Delta kl = -3\pi$), the pulse width was compressed to be about 5 ps, however the CW mode locking threshold was relatively high (0.146 μJ).

Without the inverse absorption, Eq. (1) predicts a critical energy of $E_p = 0.153$ μJ, the experimental critical energy was about 0.174 μJ. With the phase matched BIBO ($\eta = 1$), Eq. (3) predicts a critical energy of $E_p = 0.058$ μJ, the experimental result was about 0.066 μJ. With the phase mismatched BIBO ($\frac{1}{2}\Delta kl = -2.5\pi, \eta = 0.0162$), Eq. (3) predicts a critical energy of $E_p = 0.092$ μJ, the experimental result was about 0.086 μJ. With another phase mismatched BIBO ($\frac{1}{2}\Delta kl = -3\pi, \eta = 0$), Eq. (3) predicts a critical energy of $E_p = 0.153$ μJ, the experimental result was about 0.146 μJ. In conclusion, the experimental results were consistent with our theoretical analysis.

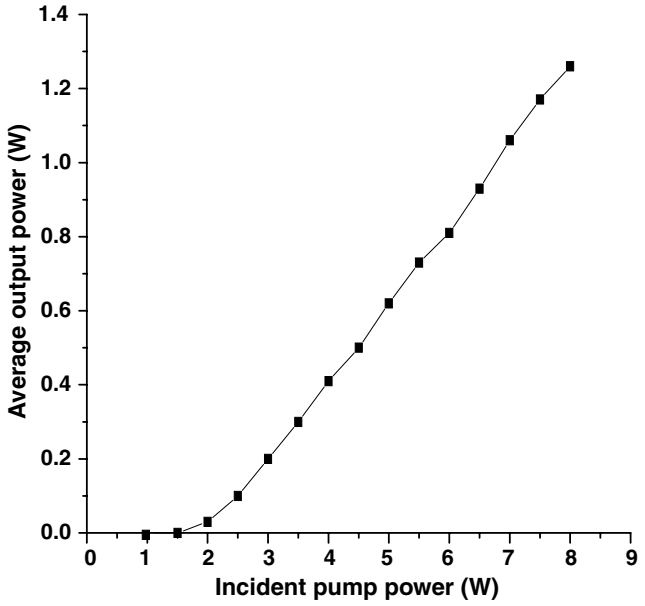

Fig. 4. The average output power as a function of incident pump power.

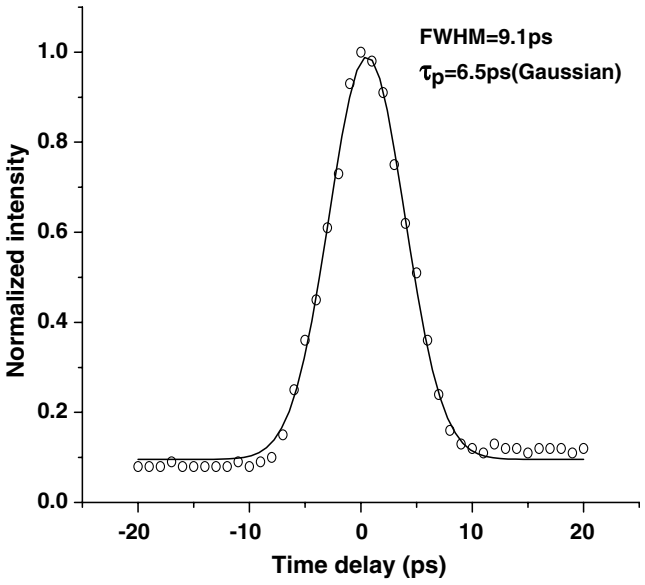

Fig. 5. Autocorrelation trace of the output pulses from the mode-locked Nd:$GdVO_4$ laser.

4. Conclusion

We have demonstrated a passively mode-locked Nd:$GdVO_4$ laser with a SESAOC. For suppressing the Q-switching stabilities and reducing the CW mode-locking threshold, a BIBO SHG crystal was used to introduce the inverse saturable absorption. With the phase matched BIBO, the Q-switching stabilities was suppressed, but the pulse width was broadened. With the phase mismatched BIBO, the CW mode-locking threshold was reduced and the pulse width was compressed, thanks to the inverse saturable absorption and self-phase modulation introduced by the special crystal. The output average power was 1.26 W; the pulse width was 6.5 ps with 128 MHz pulse repetition rate. We also modified the equation for calculating the critical energy with mismatched SHG crystal and calculated the critical energy according to this equation. The theoretical calculations were consistent with our experimental results.

References

[1] L.R. Brovelli, U. Keller, T.H. Chiu, J. Opt. Soc. Am. B. 12 (1995) 311.
[2] L.R. Jung, F.X. Kartner, N. Metuchen, D.H. Sutter, F. Morier-Genoud, Z. Shi, V. Scheuer, M. Tilsch, T. Tschudi, U. Keller, Appl. Phys. B 65 (1997) 137.
[3] U. Keller, D.A.B. Boyd, T.H. Chiu, J.F. Ferguson, T. Asom, Opt. Lett. 17 (1992) 505.
[4] Y.F. Chen, S.W. Tsai, Y.P. Lan, S.C. Wang, K.F. Huang, Opt. Lett. 26 (2001) 199.
[5] J.L. He, Y.X. Fan, J. Du, Y.G. Gang, S. Liu, H.T. Wang, L.H. Zhang, Y. Huang, 29 (2004) 2803.
[6] S.J. Zhang, E. Wu, H.F. Pan, H.P. Zeng, IEEE J. Quantum Electron. 40 (2004) 505.
[7] Y.G. Wang, X.Y. Ma, Y.X. Fan, H.T. Wang, Appl. Opt. 44 (2005) 4384.
[8] B.Y. Zhang, G. Li, M. Chen, H.J. Yu, Y.G. Wang, X.Y. Ma, Opt. Commun. 244 (2005) 311.
[9] Y.L. Jia, Z.Y. Wei, J.A. Zheng, W.J. Ling, Y.G. Wang, X.Y. Ma, Z.G. Zhang, Chin. Phys. Lett. 21 (2004) 2209.
[10] C. Honninger, R. Paschotta, F. Morier-genoud, M. Moser, U. Keller, J. Opt. Soc. Am. B. 16 (1999) 46.
[11] P. Cerny, G. Valentine, D. Burns, K. Mcewan, Opt. Lett. 29 (2004) 1387.
[12] A. Agnesi, A. Guandalini, A. Tomaselli, E. Sani, A. Toncelli, M. Tonelli, Opt. Lett. 29 (2004) 1638.
[13] T.R. Schibli, E.R. Thoen, F.X. Kartner, E.P. Ippen, Appl. Phys. B. 70 (2000) S41.
[14] R. Desalvo, D.J. Hagan, M. Sheik-bahae, G. Stegeman, E.W. van stryland, H. Vanherzeele, Opt. Lett. 17 (1992) 28.
[15] R. Paschotta, U. Keller, Appl. Phys. B. 73 (2001) 653.
[16] S.L. Schieffer, D. Brajkovic, A.I. Cornea, W. Andreas Schroeder, Opt. Express. 14 (2006) 6694.